

Mechanistic Details of Pd(II)-Catalyzed C–H Iodination with Molecular I₂: Oxidative Addition vs Electrophilic Cleavage

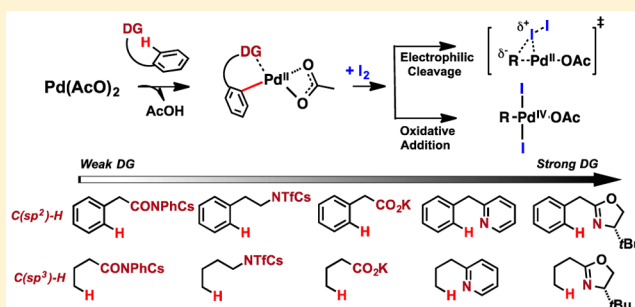
Brandon E. Haines,[†] Huiying Xu,^{†,§} Pritha Verma,[‡] Xiao-Chen Wang,[‡] Jin-Quan Yu,^{*,‡} and Djameladdin G. Musaev^{*,†}

[†]Cherry L. Emerson Center for Scientific Computation, Emory University, 1515 Dickey Drive, Atlanta, Georgia 30322, United States

[‡]Department of Chemistry, The Scripps Research Institute, 10550 North Torrey Pines Road, La Jolla, California 92037, United States

Supporting Information

ABSTRACT: Transition metal-catalyzed C–H bond halogenation is an important alternative to the highly utilized directed-lithiation methods and increases the accessibility of the synthetically valuable aryl halide compounds. However, this approach often requires impractical reagents, such as IOAc, or strong co-oxidants. Therefore, the development of methodology utilizing inexpensive oxidants and catalyst containing earth-abundant transition metals under mild experimental conditions would represent a significant advance in the field. Success in this endeavor requires a full understanding of the mechanisms and reactivity governing principles of this process. Here, we report intimate mechanistic details of the Pd(II)-catalyzed C–H iodination with molecular I₂ as the sole oxidant. Namely, we elucidate the impact of the: (a) Pd-directing group (DG) interaction, (b) nature of oxidant, and (c) nature of the functionalized C–H bond [C(sp²)–H vs C(sp³)–H] on the Pd(II)/Pd(IV) redox and Pd(II)/Pd(II) redox-neutral mechanisms of this reaction. We find that both monomeric and dimeric Pd(II) species may act as an active catalyst during the reaction, which preferentially proceeds via the Pd(II)/Pd(II) redox-neutral electrophilic cleavage (EC) pathway for all studied substrates with a functionalized C(sp²)–H bond. In general, a strong Pd–DG interaction increases the EC iodination barrier and reduces the I–I oxidative addition (OA) barrier. However, the increase in Pd–DG interaction alone is not enough to make the mechanistic switch from EC to OA: This occurs only upon changing to substrates with a functionalized C(sp³)–H bond. We also investigated the impact of the nature of the electrophile on the C(sp²)–H bond halogenation. We predicted molecular bromine (Br₂) to be more effective electrophile for the C(sp²)–H halogenation than I₂. Subsequent experiments on the stoichiometric C(sp²)–H bromination by Pd(OAc)₂ and Br₂ confirmed this prediction. The findings of this study advance our ability to design more efficient reactions with inexpensive oxidants under mild experimental conditions.



(a) Pd-directing group (DG) interaction, (b) nature of oxidant, and (c) nature of the functionalized C–H bond [C(sp²)–H vs C(sp³)–H] on the Pd(II)/Pd(IV) redox and Pd(II)/Pd(II) redox-neutral mechanisms of this reaction. We find that both monomeric and dimeric Pd(II) species may act as an active catalyst during the reaction, which preferentially proceeds via the Pd(II)/Pd(II) redox-neutral electrophilic cleavage (EC) pathway for all studied substrates with a functionalized C(sp²)–H bond. In general, a strong Pd–DG interaction increases the EC iodination barrier and reduces the I–I oxidative addition (OA) barrier. However, the increase in Pd–DG interaction alone is not enough to make the mechanistic switch from EC to OA: This occurs only upon changing to substrates with a functionalized C(sp³)–H bond. We also investigated the impact of the nature of the electrophile on the C(sp²)–H bond halogenation. We predicted molecular bromine (Br₂) to be more effective electrophile for the C(sp²)–H halogenation than I₂. Subsequent experiments on the stoichiometric C(sp²)–H bromination by Pd(OAc)₂ and Br₂ confirmed this prediction. The findings of this study advance our ability to design more efficient reactions with inexpensive oxidants under mild experimental conditions.

INTRODUCTION

Transition metal-catalyzed C–H bond halogenation^{1,2} is complementary to the highly utilized directed-lithiation methods³ and increases the accessibility of the synthetically valuable aryl halide compounds (Ar-X, X = Cl, Br and I).^{1,2} However, this method often requires impractical reagents, such as IOAc,⁴ or strong co-oxidants.^{1b,5} Therefore, the recent reports of Pd(II)-catalyzed *ortho*-directed C–H iodination (see Figure 1)⁶ as well as desymmetrization⁷ and kinetic resolution⁸ variants with inexpensive I₂ under mild experimental conditions represent a significant advance in the field.⁹

While a key feature of these reactions is believed to be the complementary bonding abilities of the employed directing groups (DG = CONHAr, NHTf, CO₂H) and auxiliary ligands,¹⁰ many mechanistic details remain unknown. Full understanding of the fundamental principles governing the reactivity and selectivity of these important reactions could significantly advance our ability to (a) design more efficient reactions through the development of inexpensive oxidants and

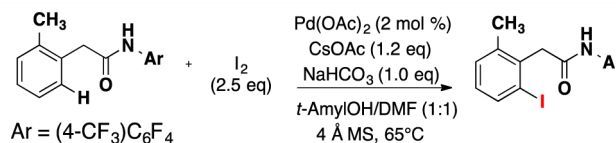


Figure 1. Reaction conditions for Pd(II)-catalyzed C–H iodination with I₂.

mild experimental conditions and (b) develop analogous processes with earth-abundant transition-metal catalysts for direct halogenation of aryl and alkyl C–H bonds.

In the literature, several possible mechanisms for C–H functionalization with aryl or alkyl-Pd(II) intermediates [R-Pd(II)] have been proposed.^{10,11} Oxidation of the R-Pd(II) species to form a R-Pd(IV) intermediate (i.e., Pd(II)/Pd(IV) redox chemistry) is one of the accepted pathways for [R-

Received: April 1, 2015

Published: July 2, 2015

Pd(II)]-mediated transformations.^{12,13} The emergence of suitable oxidants and ligands allowing the isolation and characterization of relevant Pd(IV) species has provided significant support to the development of Pd(II)/Pd(IV) redox chemistry.^{14,15} Notably, Pd(II)/Pd(IV) redox chemistry has been experimentally observed for halogenation¹⁶ with both molecular iodine¹⁴ and methyl iodide.^{12a,17} Furthermore, recent density functional theory (DFT) studies support the formation of proposed Pd(IV) intermediates in directed C(sp³)-H arylation with phenyl iodide¹⁸ as well as in various C-C,¹⁹ C-O,²⁰ C-N,²¹ and C-F²² bond-forming reactions. In particular, Pd(IV) intermediates are increasingly being proposed with so-called “F+” oxidants such as *N*-fluorobenzene-sulfonamide (NFSI) or Selectfluor to facilitate a variety of transformations.^{1e,23} A somewhat controversial²⁴ Pd(II)/Pd(IV) mechanism has also been suggested for the Heck reaction with P,N pincer-type ligands.²⁵

However, redox-neutral pathways for aryl or alkyl-Pd(II) reactive intermediates are also known. For example, these species react in C-C bond forming reactions with both nucleophiles, like enolates,²⁶ and with electrophiles, like carbonyl compounds.²⁷ Within this context, Bercaw and co-workers have reported concerted metalation-deprotonation (CMD)-type transition states in the electrophilic cleavage of Pd(II)-C bonds by acids.²⁸ Other mechanistic alternatives that have been reported include R-Pd(II)/R-Pd(II) transmetalation²⁹ and binuclear Pd(III)-Pd(III) intermediate formation.³⁰

These examples clearly demonstrate the multifaceted reactivity of the [R-Pd(II)] species. Extensive analysis indicates that the nature of the (a) aryl or alkyl ligands, (b) complementary interactions between the Pd-center, directing group, and auxiliary ligands, (c) oxidant, and (d) base, solvent, and cosolvent can alter the mechanism and significantly impact the reactivity and selectivity of these reactions.

Armed by the aforementioned knowledge, we launched a comprehensive study of the mechanism and governing factors of the recently reported Pd(II)-catalyzed C-H iodination with I₂ as the sole oxidant (Figure 1). We focused on studying the Pd(II)/Pd(IV) redox pathway [called oxidative addition (OA)] and a Pd(II)/Pd(II) redox-neutral pathway [called electrophilic cleavage (EC)] for the iodination step of this reaction (see Figure 2). We also examined the role of Pd(II)-Pd(II) dimer formation on these pathways. With these mechanistic scenarios in mind, we turned to understanding the influence of the (a) Pd-DG interaction, (b) nature of oxidant, and (c) nature of the functionalized C-H bond [C(sp²)-H vs C(sp³)-H] on the mechanistic details of halogenation of the C-H activated product complex [R-Pd(II)].

We expect that this study will illuminate the intimate details of the Pd(II)-catalyzed halogenation of aryl and alkyl C-H bond by inexpensive oxidant I₂. This, in turn, will advance our ability to design more efficient Pd(II) and earth-abundant transition-metal catalysts for C-H halogenation with inexpensive oxidants and mild experimental conditions.

METHODS

Computational Details. Calculations were performed with the Gaussian 09 (G09) program.³¹ All reported structures were fully optimized (without geometry constraint) at the M06/[6-31G(d,p) + LanL2dz (Pd, Cs, I, Br)] level of theory with the corresponding effective core potential for Pd, Cs, I, and Br.³² Single point energy calculations of selected intermediates and transition states of the reaction are performed at the M06/[[6-311+G(d,p)] + SDD (Pd, Cs,

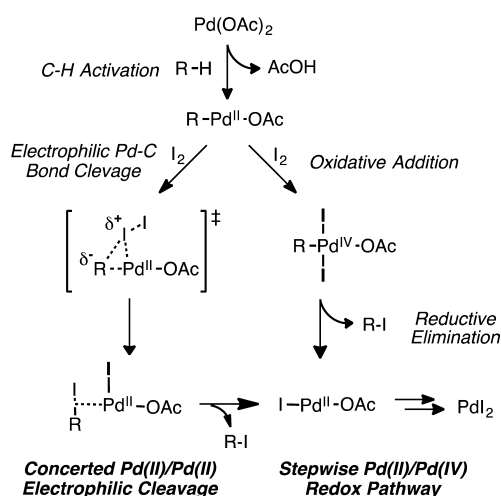


Figure 2. Schematic presentation of the oxidative addition Pd(II)/Pd(IV) and Pd(II)/Pd(II) electrophilic cleavage pathways of the Pd(II)-catalyzed C-H bond iodination by I₂ oxidant.

I)] level of theory with the corresponding effective core potentials for Pd, Cs, and I (see Supporting Information, SI).³³ These methods are denoted M06/BS1 and M06/BS2//M06/BS1, respectively. All presented geometries and energies incorporate solvent effects [N,N-dimethylformamide (DMF) is used as the solvent] calculated at the self-consistent reaction field polarizable continuum model (IEF-PCM)³⁴ level.

Frequency calculations were performed at the M06/BS1 level of theory to confirm the nature of the reported structures and to calculate enthalpy and entropy corrections under standard conditions (1 atm and 298.15 K). One should emphasize that the used PCM approach inadequately describes entropy in the solution phase due to the suppression of translational component of the entropy upon moving from the gas phase to a solvent. Despite the availability of numerous methods for correcting this error,³⁵ in this paper we decided to use only PCM Gibbs free energies and enthalpies because they are effective for comparison of relative free energies. Intrinsic reaction coordinate (IRC) calculations were performed for representative transition states to ensure that they connect the appropriate reactant and product. NBO analysis was performed for selected structures with the NBO program (version 3.1), as implemented in G09.³⁶

Experimental Details. A 25 mL pressure tube equipped with a magnetic stir bar was charged with *o*-methyl phenylacetic amide substrate (0.30 mmol), Pd(OAc)₂ (67.4 mg, 0.30 mmol), CsOAc (69 mg, 0.36 mmol), NaHCO₃ (25 mg, 0.30 mmol), Br₂ (120 mg, 0.75 mmol), 4 Å molecular sieves (150 mg), 2.5 mL *t*-amyl alcohol and 2.5 mL DMF under air. The tube was sealed by a Teflon screw cap. The reaction mixture was sonicated for 2 min, and then stirred at 65 °C for 16 h. After being allowed to cool to room temperature, the mixture was concentrated in vacuo. Column chromatography with ethyl acetate and hexane as the eluent provided the pure brominated compound (also see Supporting Information for more details of the presented kinetic experiments).

RESULTS AND DISCUSSION

Catalysis Initiation. In order to initiate the aryl C(sp²)-H iodination reaction with Pd(II) and I₂, the *N*-aryl amide substrate **A** should coordinate to the Pd(II) center of the active catalyst [Pd(OAc)₂ or its derivatives, see below] in the presence of CsOAc. Previously, we have shown that the deprotonation of the amide group of EtCONHAr by the Cs salt is necessary for its optimal coordination to the Pd(II)-center.³⁷ Joint NMR and computational data have suggested that the strong electron-withdrawing substituents on the *N*-Ar group, e.g., C₆F₅ or (4-CF₃)C₆F₄, increase the acidity of the amide N-

H bond and make the reactive deprotonated amide species widely available. After deprotonation of the substrate by the Cs⁺ counterion stays weakly coordinated to the π -electronic density of the [OCNAr]⁻ fragment.³⁸ For the sake of simplicity of computation, in this paper we employed the deprotonated substrate A-Cs, i.e., [Ph-CH₂-CONPhCs] (see Figure 3) to elucidate mechanistic details of the C-H bond iodination by Pd(II) catalyst.

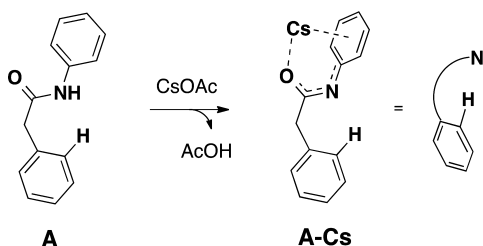


Figure 3. Deprotonation of the aryl amide substrate A by CsOAc.

As demonstrated in the literature,³⁹ homogeneous Pd(OAc)₂ can exist in various aggregate forms, including (but not limited to) monomeric, Pd(OAc)₂, dimeric, [Pd(OAc)₂]₂, or trimeric [Pd(OAc)₂]₃ species. It is possible that these forms of the Pd(II) precatalyst are individually or collectively responsible for its catalytic activity. In fact, it was shown that fine-tuning of the monomeric or dimeric forms (which could be the resting state) of the catalyst can have a large impact on the observed reactivity.⁴⁰ Therefore, at the outset of our discussion of the Pd(OAc)₂-catalyzed C-H iodination with I₂, we estimated the feasibility of these aggregate forms of Pd(OAc)₂ to be active catalytic species during the reaction (see SI for more details). Calculations show that the dimeric structure, [Pd(OAc)₂]₂, 19.2 kcal/mol more stable than two Pd(OAc)₂ monomers (Figure 4, for sake of simplicity we excluded explicit solvent

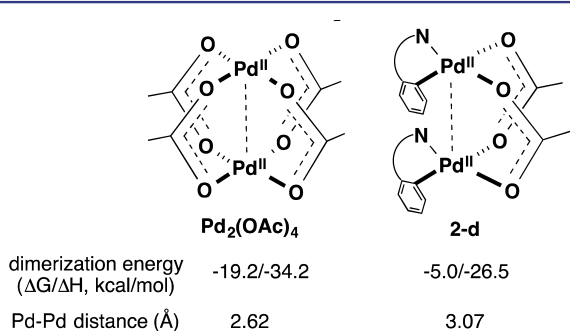


Figure 4. Possible initial dimeric Pd(II) active species. Energies are given relative to two of the corresponding monomers.

molecules from these calculations). This finding suggests that we cannot ignore the possibility of Pd(II) dimer formation and its impact on the reaction.

It is also important to keep in mind that Pd dimer formation is highly dependent on the Pd concentration in the reaction mixture. Therefore, going forward we will mostly focus on modeling the Pd(OAc)₂-catalyzed C-H iodination with I₂ with the monomeric Pd species, but will comment on the impact of Pd(II) dimer formation on the calculated energetics and reaction mechanism when necessary.

Next, coordination of the deprotonated substrate A-Cs to monomeric Pd(OAc)₂ leads to the formation of the complex

[Ph-CH₂-CONPhCs]-Pd(OAc)₂, **1**, which stabilizes the monomeric Pd form. Therefore, this is assumed to be the starting structure for the reaction (see Figure 5). It should be

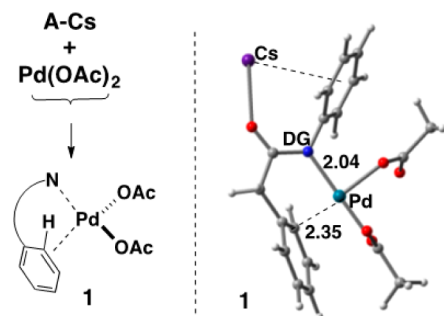


Figure 5. Formation and structural parameters of prereaction complex **1**.

noted that the dimerization of **1** to give **1-d** (see SI) is exergonic by 5.6 kcal/mol, which is much less than the dimerization energy for Pd₂(OAc)₄. (Here and below, the suffix “-d” is used to indicate the dimeric structure.)

C-H Activation. The next step of the reaction is aryl C-H bond activation that proceeds via the concerted metalation-deprotonation (CMD) mechanism.⁴¹ Initiated from the monomeric complex **1**, the calculated CMD transition state and final product (after the removal of AcOH) are **TS-H** and the square planar d⁸-Pd(II) palladacycle, **2**, respectively.

As shown in Figure 6, this step of the reaction, which is redox-neutral, requires a barrier of 14.3 kcal/mol and is

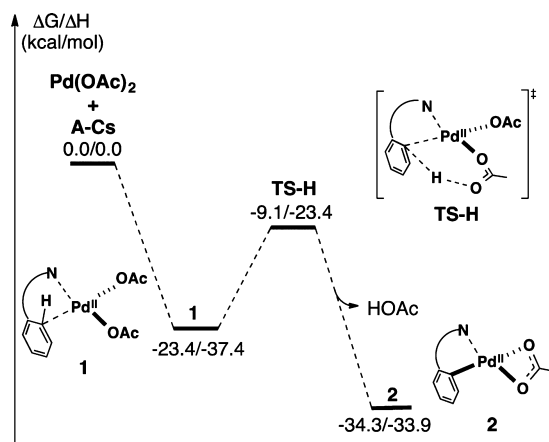


Figure 6. Schematic presentation of the potential energy surface of the C-H activation step.

exergonic by 10.9 kcal/mol (calculated relative to **1**).⁴² However, the true values of the C-H activation barrier and reaction energy are the subject of more precise selection of the reference structure. Indeed, in the reaction mixture the true nature of the reference structure is subject to the presence of coordinating ligands/solvents, the concentration of substrate, and precatalyst, among other factors. In any case, the calculated values provided in the literature, as well as in this paper, should be used either to explain trends in the C-H activation reaction or in combination with other parameters for direct comparison to experiment.⁴²

At this point, we also wish to comment on the role of exogenous base additives, which have been shown to play an

essential role in promoting the CMD step in various C–H activation reactions.⁴³ As reported in literature, a base may promote the CMD process either by ligand exchange (for example, exchange of carboxylate ligands by carbonates)⁴⁴ or by acting as a proton or acetic acid scavenger.⁴⁵

However, recent computational studies have revealed a previously unreported role for the base in C–H activation: Namely, the addition of base to the reaction mixture may also lead to formation of a stable molecular cluster with other components (substrate, ligand, solvent, etc.) of the reaction.^{37,46} This newly formed molecular cluster can promote the C–H activation step either by direct involvement in the CMD transition state or by chelating the substrate through an electrostatic cation–heteroatom interaction and altering electronic properties of the activated C–H bond.⁴⁶ In this paper, we examined the possibility of the ligand exchange and cluster formation with the exogenous base, NaHCO₃, used in the experiments. We found that neither AcO[−] → HCO₃[−] ligand exchange nor the [NaHCO₃–AcO][−] cluster formation (coordinated to the Pd-center) reduces the C–H activation barrier (see SI). Instead, it is likely that, in this reaction, the NaHCO₃ base is assisting the C–H activation step by scavenging acetic acid and driving the reaction toward the square planar d⁸-Pd(II) palladacycle, **2**, formation.^{44,45}

Previously, it has been shown (in a different system) that the dinuclear Pd complex does not have dramatic effect on the C–H activation step.⁴⁷ However, our calculations show that the dimerization of the formed palladacycle **2** to give **2-d** is favorable by 5.0 kcal/mol (see Figure 4 and SI). This finding indicates that dimer formation can play a significant role in the reaction following C–H activation.

I₂ Association. Following C–H activation is coordination of the I₂ oxidant to the d⁸-Pd(II) palladacycle, **2** (or its dimer species **2-d**). Our extensive calculations of I₂ coordination to monomer **2** resulted in two structurally and electronically different I₂ adducts, **EC-3** and **OA-3** (see Figure 7). The

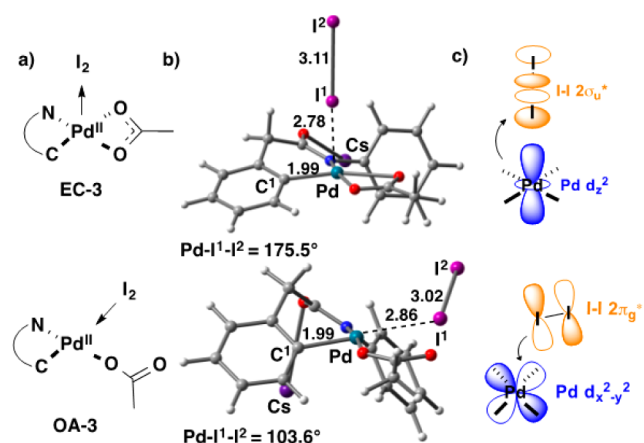


Figure 7. (a) Schematic, (b) ball-and-stick, and (c) orbital representations of the I₂–Pd(II) donor, **OA-3**, and acceptor **EC-3** complexes.

structural features of these complexes are in full agreement with nature of the iodine molecule and recent analysis of [d⁸-Pt(II)]–I₂ bonding by Rogachev and Hoffmann.⁴⁸ Briefly, the I₂ molecule, with the frontier electronic configuration of [... (1σ_g)²(1σ_u^{*})²(2σ_g)²(2π_u)⁴(2π_g^{*})⁴(2σ_u^{*})⁰] can function either as an electron acceptor (to the 2σ_u^{*} orbital) or an electron

donor (from the 2π_g^{*} orbital). As an electron-accepting ligand, the 2σ_u^{*} orbital of I₂ preferably interacts with the doubly occupied d_{z²} orbital of Pd. This 2σ_u^{*}–d_{z²} interaction (i.e., overlap) is more favorable (i.e., overlap is larger) when I₂ coordinates to the axial position of the square-planar d⁸-Pd(II) complex in a linear fashion. In contrast, as an electron-donating ligand, the HOMO (i.e., 2π_g^{*} orbital) of I₂ interacts with the empty d_{x²−y²} orbital of Pd. This orbital interaction is maximized when I₂ coordinates to an equatorial position of the square-planar d⁸-Pd(II) complex in a bent conformation.

In the energetically more stable **EC-3** complex, the Pd(d_{z²}) → I₂(2σ_u^{*}) electron donation is evident by the elongation of the I¹–I² bond (from 2.84 Å in free molecular iodine to 3.11 Å in complex **EC-3**) and the calculated ∠Pd–I¹–I² angle of 175.5°. It is important to emphasize that, due to the inherent electronic nature of square-planar d⁸-Pd(II), (a) bent coordination of I₂ at the axial position is highly unstable, and (b) I₂ is the only ligand present in the C–H iodination reaction mixture (including DMF, CsOAc, AcOH and *t*-amyl-OH) that forms a favorable axial interaction (ΔG_{bind} = −11 kcal/mol) with the Pd(II)-center of **2** (see SI for more details).

On the other hand, in complex **OA-3**, I₂ acts as an electron donor (from the 2π_g^{*} orbital), which is manifested in its bent coordination (∠Pd–I¹–I² = 103.6°) (see Figure 7). The lower stability (by 6.5 kcal/mol) of the I₂ (donor, 2π_g^{*}) → Pd(acceptor, d_{x²−y²}) complex (**OA-3**) compared to the Pd(donor, d_{z²}) → I₂(acceptor, 2σ_u^{*}) complex (**EC-3**) is shown to arise from the smaller energy gap between the Pd(d_{z²}) and I₂(2σ_u^{*}) orbitals compared to the I₂(2π_g^{*}) and Pd(d_{x²−y²}) orbitals (see SI). We expect that the energetically less favorable complex **OA-3** can easily rearrange to complex **EC-3**. Extensive computations show that the (**OA-3**) → (**EC-3**) transformation requires a barrier of only 5.5 kcal/mol and proceeds via the dissociation of I₂ from **OA-3** and subsequent re-coordination to the axial position of the Pd-center in **EC-3**.

Coordination of an I₂ molecule, as an acceptor ligand, to the dimer complex **2-d** forms **EC-3-d** intermediate (see Figure 8).

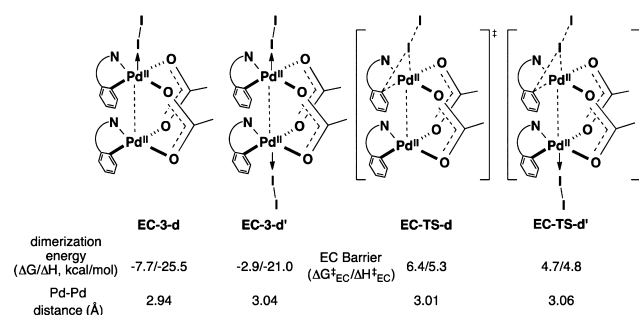


Figure 8. Possible dimeric Pd(II)–I₂ donor–acceptor complexes on the EC pathway. **EC-3-d** and **EC-3-d'** are mono- and di-I₂ complexes, respectively, and the dimerization energy is calculated relative to the corresponding monomers. The EC barriers for transition states **EC-TS-d** and **EC-TS-d'** are calculated relative to **EC-3-d** and **EC-3-d'**, respectively.

This process is calculated to be 13.7 kcal/mol exergonic, which is ca. 2.7 kcal/mol larger than that of the I₂ coordination to the monomer. Close examination of the geometries of the corresponding product complexes **EC-3** and **EC-3-d** reveals that this 2.7 kcal/mol stabilization is a result of strengthening the Pd–Pd interaction in complex **EC-3-d**. Indeed, the calculated Pd–Pd distance is shorter in complex **EC-3-d**

(2.94 Å) than in complex **2-d** (3.07 Å), which has no ligands at the axial position. These data suggest that the overlap between the $\text{Pd}(d_z^2)\text{-Pd}(d_z^2)$ orbitals increases when I_2 coordinates to the Pd-center. This is another manifestation of the electron-accepting nature of the I_2 molecule in these complexes and is consistent with the crystal structure of the Pd(II) dimer donor–acceptor complex with electron-acceptor ligand tetra-cyanoethylene reported by Ritter.⁴⁹

Coordination of a second I_2 molecule to **EC-3-d** is exergonic by 6.6 kcal/mol and produces complex **EC-3-d'** (Figure 8). This indicates that the second I_2 molecule binds weaker than the first by 7.1 kcal/mol. This finding can be attributed to a significant destabilization of the Pd–Pd bond upon coordination of a second electron-accepting ligand *trans* to the first. As a result, the Pd–Pd bond distance elongates in complex **EC-3-d'** (3.04 Å) compared to complex **EC-3-d** (2.94 Å), which only has one electron-accepting ligand (I_2). Despite this, overall coordination of two I_2 molecules is thermodynamically favored. These data, once again, show that dimerization of the Pd(II) intermediates during the reaction cannot be ruled out.⁵⁰

While the electronic and geometric features of several structurally and electronically different $\text{M}(\text{acceptor}) \leftarrow \text{X}_2(\text{donor})$ and $\text{M}(\text{donor}) \rightarrow \text{X}_2(\text{acceptor})$ complexes have been the subject of several experimental^{51,52} and computational^{53,48} studies, their importance for C–H bond halogenation and for catalysis in general have not been fully explored. Therefore, below, we investigate the Pd(II)-catalyzed C–H bond iodination with I_2 by considering (a) the $\text{M}(\text{acceptor}) \leftarrow \text{X}_2(\text{donor})$ complex **OA-3** as the starting point for the Pd(II)/Pd(IV) redox process and (b) the $\text{M}(\text{donor}) \rightarrow \text{X}_2(\text{acceptor})$ complexes **EC-3** and **EC-3-d** as the initial point of the Pd(II)/Pd(II) redox-neutral process.⁵⁴

Pd(II)/Pd(IV) Redox Pathway. Starting from the complex **OA-3**, the OA of I_2 to Pd(II) occurs through an asymmetric three-centered oxidative insertion transition state, **OA-TS** (see Figure 9). The calculated free energy barrier ($\Delta G_{\text{OA}}^\ddagger$) at the

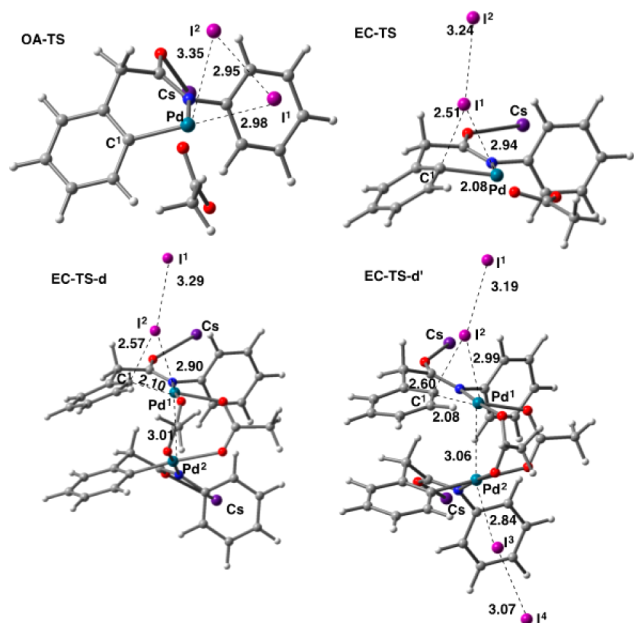


Figure 9. Important geometrical features of the oxidative addition transition state, **OA-TS**, and the electrophilic cleavage transition states, with monomeric Pd(II), **EC-TS**, and dimeric Pd(II), **EC-TS-d** and **EC-TS-d'**.

oxidative addition transition state is 14.7 kcal/mol (see Figure 10, green), and the resulting Pd(IV) intermediate **OA-4**, where I^1 is *cis* to I^2 and *trans* to C^1 , lies slightly higher in energy than starting complex **OA-3**. However, intermediate **OA-4** easily rearranges to the more stable isomer **OA-5**, where I^1 is *trans* to the DG. As a result, the overall I–I oxidative addition to Pd(II) center becomes thermodynamically favorable by ca. 13 kcal/mol. The following $\text{C}^1\text{-I}^1$ reductive elimination from **OA-5** occurs with a 10.6 kcal/mol barrier (through the transition state **OA-TSRE**) and leads to complex **6**, which consists of the iodinated substrate (**A-I**) coordinated to $\text{IPd}(\text{OAc})$. Thus, the rate-limiting barrier of the two-electron oxidation by I_2 is 14.7 kcal/mol (at the I–I oxidative addition transition state **OA-TS**), and the overall C–H iodination step (**OA-3** \rightarrow **6**) is exergonic by 18.4 kcal/mol.

Another possible mechanism for oxidative addition is $\text{S}_{\text{N}}2$ attack on I_2 by the Pd atom.⁵⁵ Despite our extensive efforts we were not able to locate any transition state associated with the oxidative addition of I_2 via the $\text{S}_{\text{N}}2$ pathway (see SI for more details). We also were unable to locate a stationary point for the $\text{S}_{\text{N}}2$ oxidative addition product complex, $[\text{Pd}(\text{IV})\text{-I}]^+$ and I^- . This is consistent with the results by Bercaw and co-workers, who were unable to locate $[\text{Pd}(\text{IV})\text{-H}]^+$ structures in studying the protonolysis of Pd(II)–C bonds.²⁸ The separated oxidation products, $[\text{Pd}(\text{IV})\text{-I}]^+$ and I^- , are 12.9 kcal/mol higher in energy than **EC-3**. This taken with the lack of a transition state indicates that the $\text{S}_{\text{N}}2$ oxidative addition pathway is unlikely with substrate **2**. We therefore focus discussion on oxidative addition through the oxidative insertion transition state.

Electrophilic Cleavage Pathway. Alternatively, the EC pathway is initiated from the $\text{Pd}(\text{donor}, d_z^2) \rightarrow \text{I}_2(\text{acceptor}, 2\sigma_u^*)$ complexes **EC-3** and/or **EC-3-d** and **EC-3-d'** and proceeds by $\text{I}^1\text{-I}^2$ electrophilic attack on the Pd– C^1 bond. Transition states associated with this process in the monomeric and dimeric complexes are **EC-TS**, **EC-TS-d**, and **EC-TS-d'**, respectively. As displayed in Figure 9, in these transition states the terminal iodide (I^2) is expelled and the proximal iodide (I^1) is engaged in bonding with the Pd and C^1 centers. The calculated free energy barrier ($\Delta G_{\text{EC}}^\ddagger$) for the monomeric active catalyst (see Figure 10, blue) is only 8.3 kcal/mol, which is much smaller than the energy required for (a) C–H activation (14.3 kcal/mol) and (b) iodination through the Pd(II)/Pd(IV) pathway (14.7 kcal/mol). The EC step is calculated to be exergonic by 2.1 kcal/mol, and presumably the resulting intermediate, **EC-4**, will also easily rearrange to the thermodynamically more stable product **6**.

The calculated EC barrier at the dimeric transition states **EC-TS-d** and **EC-TS-d'** are 6.4 and 4.7 kcal/mol, respectively (Figure 8). These barriers are 0.9 and 3.7 kcal/mol smaller than that for the monomeric case indicating that the Pd(II)–Pd(II) dimer facilitates the electrophilic cleavage step. Comparison of the geometry parameters of transition states **EC-TS**, **EC-TS-d**, and **EC-TS-d'** shows that they are very similar (Figure 9). Therefore, the observed stabilization of the dimeric EC transition state is expected to come from the Pd–Pd interaction. Indeed, the calculated Pd–Pd bond length in the dimeric transition states (3.01 and 3.06 Å) are slightly shorter than prior to I_2 coordination (**2-d**, 3.07 Å) but longer than that in the I_2 adducts (2.94 and 3.04 Å)⁵⁶ (see Figures 4 and 8). Following EC at **EC-TS-d'**, a second EC reaction can occur at Pd^2 with a barrier of 10.1 kcal/mol. This barrier is higher than the first one likely because it occurs at the concave face of the palladacycle (see SI).

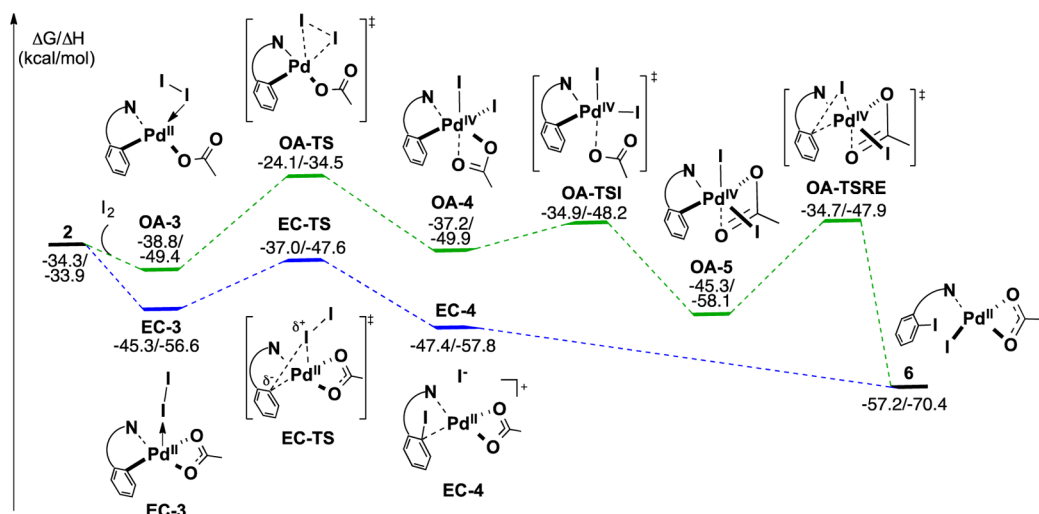


Figure 10. Potential energy surface for C–H iodination via the Pd(II)/Pd(IV) redox (green) and the electrophilic cleavage Pd(II)/Pd(II) redox-neutral (blue) pathways. The reported energies are calculated relative to Pd(OAc)₂ and A-Cs.

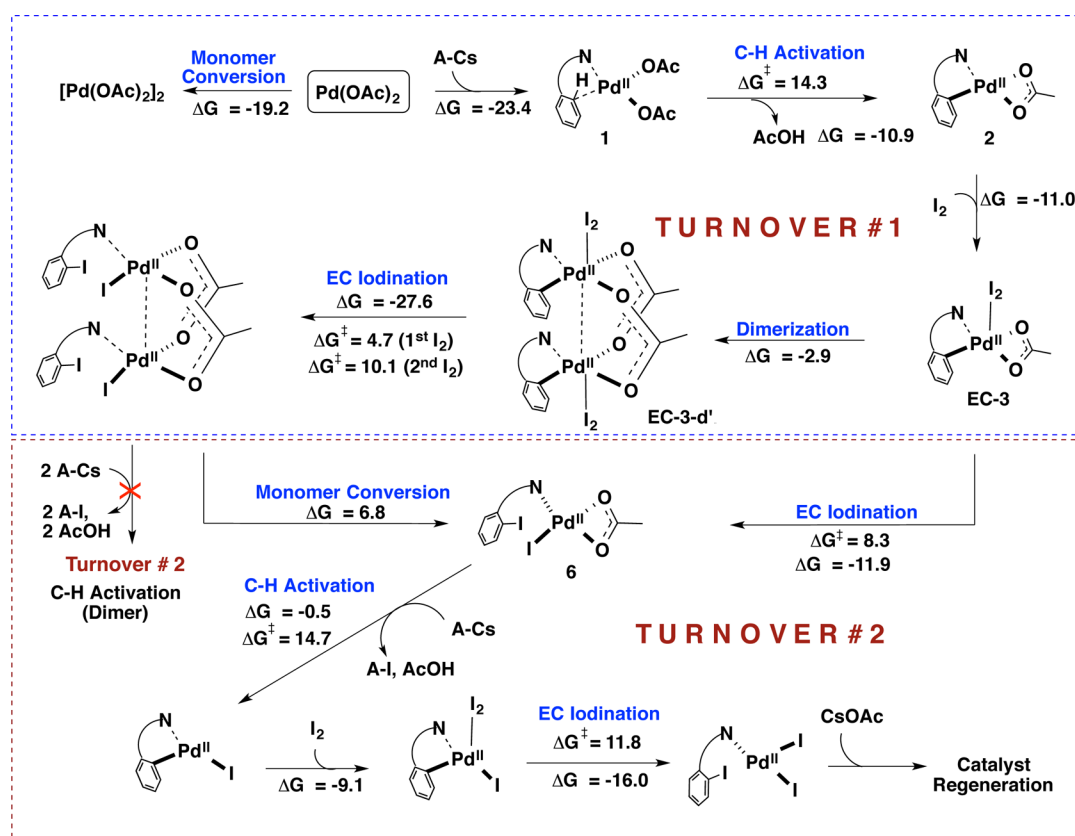


Figure 11. C–H iodination pathway proceeding through the EC mechanism and including Pd(II) dimer formation.

Second Turnover. As illustrated in Figure 10, the aforementioned OA and EC stoichiometric pathways with monomeric Pd(OAc)₂ lead to the same IPd(OAc) complex, **6**, which could act as an active species for a second C–H iodination reaction. The calculated C–H activation, I–I oxidative addition, and I₂ electrophilic cleavage barriers are 14.7, 13.1, and 11.8 kcal/mol, respectively, with monomeric IPd(OAc) (see SI for the full potential energy surface). Comparison of these energy values with those reported above for Pd(OAc)₂ shows that the processes initiated by monomeric Pd(OAc)₂ and IPd(OAc) active species proceed via comparable

energy barriers. This finding suggests that both the EC and Pd(II)/Pd(IV) pathways will lead to the unreactive PdI₂ product after two catalyst turnovers (see SI), if the reaction will be catalyzed by the monomeric active species. Therefore, regeneration of Pd(OAc)₂ or IPd(OAc) from PdI₂ (with CsOAc in this case) becomes absolutely necessary for catalyst turnover. Our mechanistic studies of this step of the reaction are in progress and will be reported later.

Furthermore, the above presented data indicate that the stoichiometric EC C–H iodination of two *N*-aryl amide substrates (2 A-Cs → 2 A-I) by the dimeric complex EC-3-d

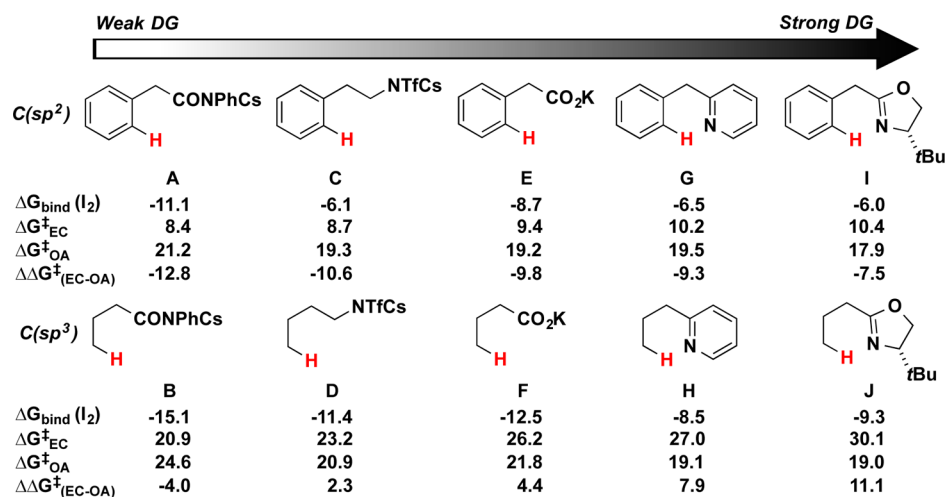


Figure 12. I₂ binding free energy (ΔG_{bind}), the free energy barriers for the EC [Pd(II)/Pd(II)] pathway ($\Delta G_{\text{EC}}^\ddagger$), OA [Pd(II)/Pd(IV)] pathway ($\Delta G_{\text{OA}}^\ddagger$), and their difference ($\Delta\Delta G_{\text{EC-OA}}^\ddagger$) for the examined C(sp²)-H and C(sp³)-H substrates with DGs of increasing strength from left to right. All energies are reported in kcal/mol. DG strength is based on experimental definition and NBO calculations (see SI).

leads to the formation of dimeric [IPd(OAc)]₂ species. While this species is stable by 11.7 kcal/mol relative to two free IPd(OAc) monomers, it cannot effectively participate in the next C-H activation process as a stable structure. Indeed, the expected CMD process for the next C-H activation is required to utilize one of the bridging acetate ligands, which will significantly destabilize the Pd(II)-Pd(II) dimer. As a consequence, we expect the dimeric pathway to merge with the monomeric pathway at this point in the reaction. In other words, the EC C-H iodination is predicted to be initiated through C-H activation by monomeric Pd(OAc)₂, proceed through a dimeric Pd intermediate that facilitates the iodination step via the EC mechanism, and ultimately lead to the formation of an active monomeric IPd(OAc) catalyst. The entire process is summarized in Figure 11. Later species complete the stoichiometric reaction through iodination of one more C-H substrate via the EC mechanism and the formation of unreactive Pd₂ species.

Thus, (a) both monomeric and dimeric Pd(II) species can act as an active catalyst in the electrophilic C-H iodination process, (b) the rate-determining step of this overall stoichiometric C-H iodination reaction is the C-H bond activation, and (c) the iodination of the C-H bond preferentially occurs via the EC mechanism regardless of monomeric or dimeric active species involvement. One should emphasize that even though the oxidative addition pathway is shown to be less likely than the EC pathway for the presented reaction, the calculated OA barriers are not prohibitively high, which suggests the general feasibility of both pathways.

After elucidating the mechanism of the aryl C(sp²)-H bond iodination by Pd(II)-catalyst and I₂ oxidant, we turned our attention to elaborating on the roles of the: (a) Pd-DG interaction, (b) nature of the functionalized C-H bond [C(sp²)-H vs C(sp³)-H], and (c) nature of oxidant (or electrophile), on the important structural and energetic aspects of the reported OA and EC pathways. For the sake of simplicity, we will use the process involving one I₂ molecule and monomeric [R-Pd(II)] reactive species for the remainder of the analysis.

SUBSTRATE EFFECT

At first we briefly discuss the impact of the nature of Pd-DG interaction to the aryl C(sp²)-H iodination mechanism. For this reason, we investigated a series of substrates with commonly employed DGs (see Figure 12). Interestingly, for all studied C(sp²)-H substrates the EC iodination pathway is more favorable than the oxidative addition pathway. In general, it is found that increasing the DG donor ability (a) reduces the I₂ coordination energy to the Pd(II) center, (b) increases of the electrophilic iodination barrier, and (c) reduces the I-I oxidative addition barrier. These trends are in good agreement with the increase in the energy difference between the Pd(d_{z²) and I₂(2σ*) orbitals and decrease in the energy difference between the Pd(d_{x²-y²) and I₂(2π*) orbitals. Close examination of the orbital energies indicates that this effect arises from increasing stabilization of the Pd(d_{z²) and Pd(d_{x²-y²) orbitals due to the increasing electron donation from the DG to the Pd-center (see SI).}}}}

The aforementioned trends for C(sp²)-H substrates also hold for the C(sp³)-H substrates. However, the calculated OA and EC barriers are significantly higher for the C(sp³)-H substrates. For example, the difference in barriers for the oxazoline DG (substrates I and J) is 19.7 kcal/mol. This finding can be explained in terms of the well-established directionality of the C(sp³)-Pd bond compared to C(sp²)-Pd bond (see SI).

It is noteworthy that for all studied C(sp³)-H substrates, only the weakest DG (B, DG = CONPhCs) would proceed via the EC pathway. For example, the experimentally active oxazoline DG in substrate J will promote the formation of a Pd(IV) intermediate for C(sp³)-H substrates, and the EC pathway is disfavored by 11.1 kcal/mol. This constitutes a switch in the mechanism from EC to OA based on the DG and nature of the functionalized C-H bond. This finding allows us to design a better catalyst for various C-H bond iodinations.

ELECTROPHILE SCOPE

Next, we investigate the effect of the nature of electrophile (E) to the reported mechanisms of the C(sp²)-H bond halogenation of substrate A. For this purpose, we calculated the electronic structure of numerous oxidants as well as their

coordination energy to monomeric complex **2** (ΔG_{bind}) and EC barrier ($\Delta G_{\text{EC}}^{\ddagger}$) for halogenation (see SI). As shown in Table 1, the calculated values of ΔG_{bind} and $\Delta G_{\text{EC}}^{\ddagger}$ correlate with the

Table 1. Comparison the $2\sigma^*$ Energies of Various Electrophiles with the Calculated Binding Energy (ΔG_{bind}) and Corresponding EC Barrier ($\Delta G_{\text{EC}}^{\ddagger}$)^a

electrophile (E)	$2\sigma^*$ orbital (eV)	ΔG_{bind} (kcal/mol)	$\Delta G_{\text{EC}}^{\ddagger}$ (kcal/mol)
ICH ₃	5.54	–	–
ICN	4.69	0.9	24.3
NIS	4.13	0.5	17.3
IOAc	3.37	–3.9	9.9
Cl ₂	2.90	–4.2	8.8
I ₂	1.83	–11.1	8.3
Br ₂	1.43	–16.1	7.7

^aThe $2\sigma^*$ orbital energies are calculated relative to the Pd(d_z^2) orbital of complex **2**.

energy level of the $2\sigma^*$ orbital, which is the orbital that is involved in the linear coordination of the electrophile to the Pd-center and the EC transition state. Consistent with the data reported above, an increase in the $2\sigma^*$ orbital energy leads to smaller ΔG_{bind} and larger $\Delta G_{\text{EC}}^{\ddagger}$ values.

Molecular bromine (Br₂) is the only electrophile for which the calculated $2\sigma^*$ orbital energy is lower in energy than that for I₂. Therefore, one may expect that Br₂ will be a suitable electrophile for C–H bromination without external oxidants. The calculations also suggest that bromination with Br₂ will react faster through the EC pathway than iodination with I₂.

Satisfyingly, the following experiments support these computational predictions. Indeed, at first, we have found that the stoichiometric C–H bromination of the *o*-methyl phenylacetic acid-derived *N*-2,3,5,6-tetrafluoro-4-trifluoromethylphenylamide occurs in 95% yield when Br₂ is used in place of I₂ under the previously reported C–H iodination conditions⁶ (Figure 13). The catalytic version of this bromination protocol is currently under investigation.

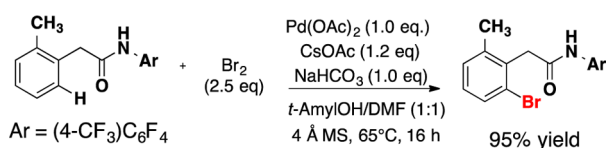


Figure 13. Reaction conditions and reaction yield for C–H bromination with stoichiometric Pd(OAc)₂.

Second, in order to validate our computational prediction that Br₂ may react faster than I₂, we performed series of kinetic experiments by subjecting the *in situ* generated palladacycle intermediate to iodine and bromine, respectively. We found that even at –50 °C, the palladacycle intermediate reacted within 30 s to give the respective products in quantitative yields. This finding: (a) indicates that bromination of C–H bond is as facile as iodination, as was predicted by our computation, (b) demonstrates that the iodination/bromination step is not likely to be the turnover-limiting step for overall catalytic reaction, and (c) prevents (unfortunately) the measurement of any kinetic data (see Figures S16 and S17, and related text in SI for more details).

Other common electrophiles, such as IOAc and *N*-iodosuccinimide (NIS), have higher-lying $2\sigma^*$ orbitals than I₂

and therefore form weaker interactions with the Pd(d_z^2) orbital and have higher EC barriers. However, for both of these reagents, the EC pathway is calculated to be lower in energy than oxidative addition ($\Delta\Delta G_{\text{EC-OA}}^{\ddagger} = -11.1$ and -14.1 kcal/mol, respectively). This indicates that the EC mechanism is general for a wide range of halogen electrophiles capable of reacting with aryl and alkyl-Pd(II) intermediates. Consistent with the above analysis, methyl iodide (ICH₃) has a high-lying σ^* orbital and has been shown experimentally to react through a Pd(II)/Pd(IV) pathway.^{12a,17,55}

CONCLUSION

The intimate details of the Pd(II)-catalyzed C–H iodination by I₂ oxidant were elucidated. We focused on studying the factors impacting the feasibility of the Pd(II)/Pd(IV) redox (OA) and Pd(II)/Pd(II) redox-neutral (EC) mechanisms of this reaction. The EC mechanism is dictated by the formation of a unique Pd(donor, d_z^2) → I₂(acceptor, $2\sigma^*$) complex. It was shown that both monomeric and dimeric Pd(II) species may act as an active catalyst in this reaction, which preferentially proceeds via the EC mechanism for all studied substrates with a functionalized C(sp²)–H bond. We calculate that stronger DGs increase the electrophilic C–H iodination barrier and reduce the I–I oxidative addition barrier. However, the increase in Pd–DG interaction alone is not enough to make mechanism switch from EC to OA; this only occurs with the combination of strong DG and C(sp³)–H substrate.

We also investigated the impact of the nature of the electrophile on the feasibility of the reported mechanisms of the C(sp²)–H bond halogenation. To this end, we show that halogen oxidants with $2\sigma^*$ orbitals close to or below the energy level of that for I₂ can be effective electrophiles for the C(sp²)–H functionalization. One such electrophile is molecular bromine (Br₂). Following experiments on the stoichiometric C(sp²)–H bromination by Pd(OAc)₂ and Br₂ confirmed these computational predictions. Thus, the proposed computation could guide the development of future reactions with novel substrates and electrophiles.

ASSOCIATED CONTENT

Supporting Information

(1) Higher order Pd(II) structures (Figures S1, S2 and Table S1); (2) C–H activation (Figures S3 and S4); (3) axial coordination to complex **2** (Figure S5 and Table S2); (4) molecular orbital (MO) analysis of I₂ and complex **2** (Figure S6); (7) I₂ OA through the S_N2 pathway (Figures S7–S9); (8) single point energies (Table S3); (9) PES starting from PdIOAc (Figure S10); (10) other redox-neutral iodination pathways (Figure S11); (11) MO and NBO analysis of complex EC-3 (Figure S12 and Tables S4 and S5); (12) substrate effect C(sp²) vs C(sp³) on EC-TS (Figures S13 and S14); (13) ring size and steric effects (Figure S15); (14) EC FMO analysis and transition states (Table S4 and Figure S12); (15) experimental characterization and spectra; (16) SI references; (17) computational energies and frequency analysis (Tables S5–S8); (18) Cartesian coordinates for all reported structures. The Supporting Information is available free of charge on the ACS Publications website at DOI: 10.1021/jacs.5b03410.

AUTHOR INFORMATION

Corresponding Authors

*dmusaev@emory.edu

*yu200@scripps.edu

Present Address

[§]School of Chemistry and Chemical Engineering, Sun Yat-Sen University, Guangzhou 510275, P. R. China,

Notes

The authors declare no competing financial interest.

ACKNOWLEDGMENTS

This work was supported by the National Science Foundation under the CCI Center for Selective C–H Functionalization (CHE-1205646). The authors gratefully acknowledge NSF MRI-R2 grant (CHE-0958205) and the use of the resources of the Cherry Emerson Center for Scientific Computation. The authors acknowledge Dr. Travis Figg and members of the CCI Center for Selective C–H Functionalization for fruitful discussion.

REFERENCES

- (1) (a) Yu, D. G.; Gensch, T.; de Azambuja, F.; Vasquez-Céspedes, S.; Glorius, F. *J. Am. Chem. Soc.* **2014**, *136*, 17722–17725. (b) Sun, X. Y.; Shan, G.; Sun, Y. H.; Rao, Y. *Angew. Chem., Int. Ed.* **2013**, *52*, 4440–4444. (c) Schroder, N.; Wencel-Delord, J.; Glorius, F. *J. Am. Chem. Soc.* **2012**, *134*, 8298–8301. (d) Bedford, R. B.; Haddow, M. F.; Mitchell, C. J.; Webster, R. L. *Angew. Chem., Int. Ed.* **2011**, *50*, 5524–5527. (e) Engle, K. M.; Mei, T. S.; Wang, X. S.; Yu, J. Q. *Angew. Chem., Int. Ed.* **2011**, *50*, 1478–1491. (f) Lyons, T. W.; Sanford, M. S. *Chem. Rev.* **2010**, *110*, 1147–1169.
- (2) For a pioneering catalytic ortho-halogenation of azobenzene, see: (a) Fahey, D. R. *J. Organomet. Chem.* **1971**, *27*, 283–292. (b) Andrienko, O. S.; Goncharov, V. S.; Raida, V. S. *Russ. J. Org. Chem.* **1996**, *32*, 79–81.
- (3) (a) Schlosser, M. *Angew. Chem., Int. Ed.* **2005**, *44*, 376–393. (b) Snieckus, V. *Chem. Rev.* **1990**, *90*, 879–933. (c) Beak, P.; Snieckus, V. *Acc. Chem. Res.* **1982**, *15*, 306–312.
- (4) Concepcion, J. I.; Francisco, C. G.; Hernandez, R.; Salazar, J. A.; Suarez, E. *Tetrahedron Lett.* **1984**, *25*, 1953–1956.
- (5) (a) Song, B. R.; Zheng, X. J.; Mo, J.; Xu, B. *Adv. Synth. Catal.* **2010**, *352*, 329–335. (b) Wan, X. B.; Ma, Z. X.; Li, B. J.; Zhang, K. Y.; Cao, S. K.; Zhang, S. W.; Shi, Z. J. *J. Am. Chem. Soc.* **2006**, *128*, 7416–7417. (c) Dudnik, A. S.; Chernyak, N.; Huang, C. H.; Gevorgyan, V. *Angew. Chem., Int. Ed.* **2010**, *49*, 8729–8732.
- (6) Wang, X. C.; Hu, Y.; Bonacorsi, S.; Hong, Y.; Burrell, R.; Yu, J. Q. *J. Am. Chem. Soc.* **2013**, *135*, 10326–10329.
- (7) Chu, L.; Wang, X. C.; Moore, C. E.; Rheingold, A. L.; Yu, J. Q. *J. Am. Chem. Soc.* **2013**, *135*, 16344–16347.
- (8) Chu, L.; Xiao, K. J.; Yu, J. Q. *Science* **2014**, *346*, 451–455.
- (9) For stoichiometric halogenation of palladacycles, see: (a) Onishi, M.; Hiraki, K.; Iwamoto, A. *J. Organomet. Chem.* **1984**, *262*, C11–C13. (b) Carr, K.; Sutherland, J. K. *J. Chem. Soc., Chem. Commun.* **1984**, 1227–1228. (c) Baldwin, J. E.; Jones, R. H.; Najera, C.; Yus, M. *Tetrahedron* **1985**, *41*, 699–711.
- (10) Engle, K. M.; Mei, T. S.; Wasa, M.; Yu, J. Q. *Acc. Chem. Res.* **2012**, *45*, 788–802.
- (11) Musaev, D. G.; Figg, T. M.; Kaledin, A. L. *Chem. Soc. Rev.* **2014**, *43*, 5009–5031.
- (12) (a) Catellani, M.; Chiusoli, G. P. *J. Organomet. Chem.* **1988**, *346*, C27–C30. (b) Catellani, M.; Chiusoli, G. P.; Castagnoli, C. *J. Organomet. Chem.* **1991**, *407*, C30–C33. (c) Dyker, G. *Angew. Chem., Int. Ed. Engl.* **1992**, *31*, 1023–1025. (d) Dyker, G. *J. Org. Chem.* **1993**, *58*, 6426–6428. (e) Dyker, G. *Angew. Chem., Int. Ed. Engl.* **1994**, *33*, 103–105.
- (13) (a) Bonney, K. J.; Schoenebeck, F. *Chem. Soc. Rev.* **2014**, *43*, 6609–6638. (b) Canty, A. J. *Dalton Trans.* **2009**, 10409–10417. (c) Hickman, A. J.; Sanford, M. S. *Nature* **2012**, *484*, 177–185. (d) Muniz, K. *Angew. Chem., Int. Ed.* **2009**, *48*, 9412–9423. (e) Sehnal, P.; Taylor, R. J. K.; Fairlamb, I. J. S. *Chem. Rev.* **2010**, *110*, 824–889. (f) Xu, L. M.; Li, B. J.; Yang, Z.; Shi, Z. J. *Chem. Soc. Rev.* **2010**, *39*, 712–733. (g) Yu, J. Q.; Giri, R.; Chen, X. *Org. Biomol. Chem.* **2006**, *4*, 4041–4047.
- (14) Canty, A. J.; Denney, M. C.; Skelton, B. W.; White, A. H. *Organometallics* **2004**, *23*, 1122–1131.
- (15) (a) Dick, A. R.; Kampf, J. W.; Sanford, M. S. *J. Am. Chem. Soc.* **2005**, *127*, 12790–12791. (b) Whitfield, S. R.; Sanford, M. S. *J. Am. Chem. Soc.* **2007**, *129*, 15142–15143.
- (16) Vigalok, A. *Acc. Chem. Res.* **2015**, *48*, 238–247.
- (17) Byers, P. K.; Canty, A. J.; Skelton, B. W.; White, A. H. *J. Chem. Soc., Chem. Commun.* **1986**, 1722–1724.
- (18) Dang, Y. F.; Qu, S. L.; Nelson, J. W.; Pham, H. D.; Wang, Z. X.; Wang, X. T. *J. Am. Chem. Soc.* **2015**, *137*, 2006–2014.
- (19) (a) Lotz, M. D.; Remy, M. S.; Lao, D. B.; Ariafard, A.; Yates, B. F.; Canty, A. J.; Mayer, J. M.; Sanford, M. S. *J. Am. Chem. Soc.* **2014**, *136*, 8237–8242. (b) Poveda, A.; Alonso, I.; Fernandez-Ibanez, M. A. *Chem. Sci.* **2014**, *5*, 3873–3882. (c) Sharma, M.; Ariafard, A.; Canty, A. J.; Yates, B. F.; Gardiner, M. G.; Jones, R. C. *Dalton Trans.* **2012**, *41*, 11820–11828.
- (20) (a) Fu, Y.; Li, Z.; Liang, S.; Guo, Q. X.; Liu, L. *Organometallics* **2008**, *27*, 3736–3742. (b) Gary, J. B.; Sanford, M. S. *Organometallics* **2011**, *30*, 6143–6149.
- (21) Ke, Z. F.; Cundari, T. R. *Organometallics* **2010**, *29*, 821–834.
- (22) (a) Furuya, T.; Benitez, D.; Tkatchouk, E.; Strom, A. E.; Tang, P. P.; Goddard, W. A.; Ritter, T. *J. Am. Chem. Soc.* **2010**, *132*, 5922–5922. (b) Racowski, J. M.; Gary, J. B.; Sanford, M. S. *Angew. Chem., Int. Ed.* **2012**, *51*, 3414–3417.
- (23) (a) Emer, E.; Pfeifer, L.; Brown, J. M.; Gouverneur, V. *Angew. Chem., Int. Ed.* **2014**, *53*, 4181–4185. (b) Iglesias, A.; Alvarez, R.; de Lera, A. R.; Muniz, K. *Angew. Chem., Int. Ed.* **2012**, *51*, 2225–2228. (c) Sibbald, P. A.; Rosewall, C. F.; Swartz, R. D.; Michael, F. E. *J. Am. Chem. Soc.* **2009**, *131*, 15945–15951.
- (24) (a) Amatore, C.; Jutand, A. *Acc. Chem. Res.* **2000**, *33*, 314–321. (b) Batsanov, A. S.; Knowles, J. P.; Whiting, A. *J. Org. Chem.* **2007**, *72*, 2525–2532. (c) Bohm, V. P. W.; Herrmann, W. A. *Chem. - Eur. J.* **2001**, *7*, 4191–4197. (d) Jutand, A.; Pytkowicz, J.; Roland, S.; Mangeney, P. *Pure Appl. Chem.* **2010**, *82*, 1393–1402. (e) Knowles, J. P.; Whiting, A. *Org. Biomol. Chem.* **2007**, *5*, 31–44. (f) Rauf, W.; Brown, J. M. *Chem. Commun.* **2013**, *49*, 8430–8440. (g) Allolio, C.; Strassner, T. *J. Org. Chem.* **2014**, *79*, 12096–12105.
- (25) (a) Sundermann, A.; Uzan, O.; Martin, J. M. L. *Chem. - Eur. J.* **2001**, *7*, 1703–1711. (b) Vicente, J.; Arcas, A.; Julia-Hernandez, F.; Bautista, D. *Angew. Chem., Int. Ed.* **2011**, *50*, 6896–6899. (c) Blacque, O.; Frech, C. M. *Chem. - Eur. J.* **2010**, *16*, 1521–1531. (d) Bolliger, J. L.; Blacque, O.; Frech, C. M. *Chem. - Eur. J.* **2008**, *14*, 7969–7977.
- (26) (a) Bellina, F.; Rossi, R. *Chem. Rev.* **2010**, *110*, 1082–1146. (b) Culkin, D. A.; Hartwig, J. F. *Acc. Chem. Res.* **2003**, *36*, 234–245. (c) Lloyd-Jones, G. C. *Angew. Chem., Int. Ed.* **2002**, *41*, 953–956.
- (27) (a) Ma, S.; Villa, G.; Thuy-Boun, P. S.; Homs, A.; Yu, J. Q. *Angew. Chem., Int. Ed.* **2014**, *53*, 734–737. (b) Sole, D.; Fernandez, I. *Acc. Chem. Res.* **2014**, *47*, 168–179. (c) Zhang, Y. H.; Shi, B. F.; Yu, J. Q. *Angew. Chem., Int. Ed.* **2009**, *48*, 6097–6100. (d) Xia, G.; Han, X.; Lu, X. *Org. Lett.* **2014**, *16*, 6184–6187.
- (28) Bercaw, J. E.; Chen, G. S.; Labinger, J. A.; Lin, B. L. *Organometallics* **2010**, *29*, 4354–4359.
- (29) (a) Cardenas, D. J.; Martin-Matute, B.; Echavarren, A. M. *J. Am. Chem. Soc.* **2006**, *128*, 5033–5040. (b) Maestri, G.; Motti, E.; Della Ca, N.; Malacria, M.; Derat, E.; Catellani, M. *J. Am. Chem. Soc.* **2011**, *133*, 8574–8585.
- (30) (a) Canty, A. J.; Ariafard, A.; Sanford, M. S.; Yates, B. F. *Organometallics* **2013**, *32*, 544–555. (b) Powers, D. C.; Lee, E.; Ariafard, A.; Sanford, M. S.; Yates, B. F.; Canty, A. J.; Ritter, T. *J. Am. Chem. Soc.* **2012**, *134*, 12002–12009. (c) Nielsen, M. C.; Lyngvi, E.; Schoenebeck, F. *J. Am. Chem. Soc.* **2013**, *135*, 1978–1985. (d) Powers, D. C.; Benitez, D.; Tkatchouk, E.; Goddard, W. A.; Ritter, T. *J. Am. Chem. Soc.* **2010**, *132*, 14092–14103. (e) Powers, D. C.; Geibel, M. A. L.; Klein, J. E. M. N.; Ritter, T. *J. Am. Chem. Soc.* **2009**, *131*, 17050–17051. (f) Powers, D. C.; Ritter, T. *Nat. Chem.* **2009**, *1*, 302–309.
- (31) Frisch, M. J.; Trucks, G. W.; Schlegel, H. B.; Scuseria, G. E.; Robb, M. A.; Cheeseman, J. R.; Scalmani, G.; Barone, V.; Mennucci,

- B.; Petersson, G. A.; Nakatsuji, H.; Caricato, M.; Li, X.; Hratchian, H. P.; Izmaylov, A. F.; Bloino, J.; Zheng, G.; Sonnenberg, J. L.; Hada, M.; Ehara, M.; Toyota, K.; Fukuda, R.; Hasegawa, J.; Ishida, M.; Nakajima, T.; Honda, Y.; Kitao, O.; Nakai, H.; Vreven, T.; Montgomery, J. A., Jr.; Peralta, J. E.; Ogliaro, F.; Bearpark, M.; Heyd, J. J.; Brothers, E.; Kudin, K. N.; Staroverov, V. N.; Kobayashi, R.; Normand, J.; Raghavachari, K.; Rendell, A.; Burant, J. C.; Iyengar, S. S.; Tomasi, J.; Cossi, M.; Rega, N.; Millam, M. J.; Klene, M.; Knox, J. E.; Cross, J. B.; Bakken, V.; Adamo, C.; Jaramillo, J.; Gomperts, R.; Stratmann, R. E.; Yazyev, O.; Austin, A. J.; Cammi, R.; Pomelli, C.; Ochterski, J. W.; Martin, R. L.; Morokuma, K.; Zakrzewski, V. G.; Voth, G. A.; Salvador, P.; Dannenberg, J. J.; Dapprich, S.; Daniels, A. D.; Farkas, Ö.; Foresman, J. B.; Ortiz, J. V.; Cioslowski, J.; Fox, D. J. *Gaussian 09*, Revision D.01; Gaussian, Inc.: Wallingford, CT, 2009.
- (32) (a) Hay, P. J.; Wadt, W. R. *J. Chem. Phys.* **1985**, *82*, 270–283. (b) Hay, P. J.; Wadt, W. R. *J. Chem. Phys.* **1985**, *82*, 299–310. (c) Wadt, W. R.; Hay, P. J. *J. Chem. Phys.* **1985**, *82*, 284–298.
- (33) (a) Andrae, D.; Haussermann, U.; Dolg, M.; Stoll, H.; Preuss, H. *Theor. Chim. Acta* **1990**, *77*, 123–141. (b) Igelmann, G.; Stoll, H.; Preuss, H. *Mol. Phys.* **1988**, *65*, 1321–1328. (c) Vonszentpaly, L.; Fuentealba, P.; Preuss, H.; Stoll, H. *Chem. Phys. Lett.* **1982**, *93*, 555–559.
- (34) (a) Cancès, E.; Mennucci, B.; Tomasi, J. *J. Chem. Phys.* **1997**, *107*, 3032–3041. (b) Mennucci, B.; Tomasi, J. *J. Chem. Phys.* **1997**, *106*, 5151–5158. (c) Scalmani, G.; Frisch, M. J. *J. Chem. Phys.* **2010**, *132*, 114110–114124.
- (35) (a) Jindal, G.; Sunoj, R. B. *J. Am. Chem. Soc.* **2014**, *136*, 15998–16008. (b) Mammen, M.; Shakhnovich, E. I.; Deutch, J. M.; Whitesides, G. M. *J. Org. Chem.* **1998**, *63*, 3821–3830. (c) Okuno, Y. *Chem. - Eur. J.* **1997**, *3*, 212–218. (d) Plata, R. E.; Singleton, D. A. *J. Am. Chem. Soc.* **2015**, *137*, 3811–3826.
- (36) Glendenning, E. D.; Reed, A. E.; Carpenter, J. E.; Weinhold, F. *NBO*, version 3.1; University of Wisconsin: Madison, WI, 1996.
- (37) Figg, T. M.; Wasa, M.; Yu, J. Q.; Musaev, D. G. *J. Am. Chem. Soc.* **2013**, *135*, 14206–14214.
- (38) (a) Anand, M.; Sunoj, R. B. *Org. Lett.* **2011**, *13*, 4802–4805. (b) Anand, M.; Sunoj, R. B. *Organometallics* **2012**, *31*, 6466–6481. (c) Anand, M.; Sunoj, R. B.; Schaefer, H. F. *J. Am. Chem. Soc.* **2014**, *136*, 5535–5538. (d) Zhang, X. G.; Dai, H. X.; Wasa, M.; Yu, J. Q. *J. Am. Chem. Soc.* **2012**, *134*, 11948–11951.
- (39) Adrio, L. A.; Nguyen, B. N.; Guilera, G.; Livingston, A. G.; Hii, K. K. *Catal. Sci. Technol.* **2012**, *2*, 316–323.
- (40) Cook, A. K.; Sanford, M. S. *J. Am. Chem. Soc.* **2015**, *137*, 3109–3118.
- (41) (a) Biswas, B.; Sugimoto, M.; Sakaki, S. *Organometallics* **2000**, *19*, 3895–3908. (b) Davies, D. L.; Donald, S. M. A.; Macgregor, S. A. *J. Am. Chem. Soc.* **2005**, *127*, 13754–13755. (c) Garcia-Cuadrado, D.; Braga, A. A. C.; Maseras, F.; Echavarren, A. M. *J. Am. Chem. Soc.* **2006**, *128*, 1066–1067. (d) Garcia-Cuadrado, D.; de Mendoza, P.; Braga, A. A. C.; Maseras, F.; Echavarren, A. M. *J. Am. Chem. Soc.* **2007**, *129*, 6880–6886. (e) Gorelsky, S. I.; Lapointe, D.; Fagnou, K. *J. Am. Chem. Soc.* **2008**, *130*, 10848–10849. (f) Cheng, G. J.; Yang, Y. F.; Liu, P.; Chen, P.; Sun, T. Y.; Li, G.; Zhang, X. H.; Houk, K. N.; Yu, J. Q.; Wu, Y. D. *J. Am. Chem. Soc.* **2014**, *136*, 894–897. (g) Haines, B. E.; Musaev, D. G. *ACS Catal.* **2015**, *5*, 830–840.
- (42) The “outer-sphere” or external acetate pathway was found to proceed through higher barriers of 22.6 kcal/mol with free acetate anion and 22.1 kcal/mol with cesium acetate; see SI.
- (43) Ackermann, L. *Chem. Rev.* **2011**, *111*, 1315–1345.
- (44) (a) Lu, Q. Q.; Yu, H. Z.; Fu, Y. *J. Am. Chem. Soc.* **2014**, *136*, 8252–8260. (b) Lafrance, M.; Rowley, C. N.; Woo, T. K.; Fagnou, K. *J. Am. Chem. Soc.* **2006**, *128*, 8754–8756.
- (45) (a) Lian, B.; Zhang, L.; Chass, G. A.; Fang, D. C. *J. Org. Chem.* **2013**, *78*, 8376–8385. (b) Mateos, C.; Mendiola, J.; Carpintero, M.; Minguez, J. M. *Org. Lett.* **2010**, *12*, 4924–4927. (c) Sun, H. Y.; Gorelsky, S. I.; Stuart, D. R.; Campeau, L. C.; Fagnou, K. *J. Org. Chem.* **2010**, *75*, 8180–8189. (d) Rousseaux, S.; Gorelsky, S. I.; Chung, B. K. W.; Fagnou, K. *J. Am. Chem. Soc.* **2010**, *132*, 10692–10705.
- (46) Xu, H. Y.; Muto, K.; Yamaguchi, J.; Zhao, C. Y.; Itami, K.; Musaev, D. G. *J. Am. Chem. Soc.* **2014**, *136*, 14834–14844.
- (47) Sanhueza, I. A.; Wagner, A. M.; Sanford, M. S.; Schoenebeck, F. *Chem. Sci.* **2013**, *4*, 2767–2775.
- (48) Rogachev, A. Y.; Hoffmann, R. *J. Am. Chem. Soc.* **2013**, *135*, 3262–3275.
- (49) Powers, D. C.; Ritter, T. *Organometallics* **2013**, *32*, 2042–2045.
- (50) Equatorial coordination of I₂ to the Pd(II) dimer complex 2-d is expected to have a destabilizing effect because it requires displacement of at least one of the bridging acetate ligands. Therefore, this possibility was not considered further.
- (51) (a) Gossage, R. A.; Ryabov, A. D.; Spek, A. L.; Stufkens, D. J.; van Beek, J. A. M.; van Eldik, R.; van Koten, G. *J. Am. Chem. Soc.* **1999**, *121*, 2488–2497. (b) Vanbeek, J. A. M.; Vankoten, G.; Dekker, G. P. C. M.; Wissing, E.; Zoutberg, M. C.; Stam, C. H. *J. Organomet. Chem.* **1990**, *394*, 659–678. (c) Vanbeek, J. A. M.; Vankoten, G.; Smeets, W. J. J.; Spek, A. L. *J. Am. Chem. Soc.* **1986**, *108*, 5010–5011. (d) Van Koten, G. *Pure Appl. Chem.* **1990**, *62*, 1155–1159.
- (52) (a) Shaffer, D. W.; Ryken, S. A.; Zarkesh, R. A.; Heyduk, A. F. *Inorg. Chem.* **2012**, *51*, 12122–12131. (b) Makiura, R.; Nagasawa, I.; Kimura, N.; Ishimaru, S.; Kitagawa, H.; Ikeda, R. *Chem. Commun.* **2001**, 1642–1643.
- (53) Bickelhaupt, F. M.; Baerends, E. J.; Ravenek, W. *Inorg. Chem.* **1990**, *29*, 350–354.
- (54) Oxidative addition of I₂ to Pd(II) dimer is not expected to be viable because, once again, disruption of the bridging acetate ligands that expected highly destabilize the dimer structure.
- (55) (a) Bickelhaupt, F. M.; Ziegler, T. *Organometallics* **1995**, *14*, 2288–2296. (b) Byers, P. K.; Canty, A. J.; Crespo, M.; Puddephatt, R. J.; Scott, J. D. *Organometallics* **1988**, *7*, 1363–1367.
- (56) We also calculated a reasonable EC barrier of 8.5 kcal/mol for intermolecular iodination in the presence of two molecules of I₂. The difference in barrier compared to the monomeric EC barrier (0.2 kcal/mol) and excess I₂ in the reaction mixture suggests this mechanism is also possible.